

Less is More: Empowering GUI Agent with Context-Aware Simplification

Gongwei Chen¹, Xurui Zhou¹, Rui Shao^{1†}, Yibo Lyu¹, Kaiwen Zhou²,
Shuai Wang², Wentao Li², Yinchuan Li², Zhongang Qi², Liqiang Nie^{1†}

¹Harbin Institute of Technology, Shenzhen ²Huawei Noah’s Ark Lab

chengongwei@hit.edu.cn shaorui@hit.edu.cn nieliqiang@gmail.com

<https://github.com/JiuTian-VL/SimpAgent>

Abstract

The research focus of GUI agents is shifting from text-dependent to pure-vision-based approaches, which, though promising, prioritize comprehensive pre-training data collection while neglecting contextual modeling challenges. We probe the characteristics of element and history contextual modeling in GUI agent and summarize: **1) the high-density and loose-relation of element context** highlight the existence of many unrelated elements and their negative influence; **2) the high redundancy of history context** reveals the inefficient history modeling in current GUI agents. In this work, we propose a context-aware simplification framework for building an efficient and effective GUI Agent, termed **SimpAgent**. To mitigate potential interference from numerous unrelated elements, we introduce a **masking-based element pruning** method that circumvents the intractable relation modeling through an efficient masking mechanism. To reduce the redundancy in historical information, we devise a **consistency-guided history compression** module, which enhances implicit LLM-based compression through innovative explicit guidance, achieving an optimal balance between performance and efficiency. With the above components, **SimpAgent** reduces 27% FLOPs and achieves superior GUI navigation performances. Comprehensive navigation experiments across diverse web and mobile environments demonstrate the effectiveness and potential of our agent.

1. Introduction

Many current GUI agents [2, 7, 22, 33–35, 51, 60] make decisions on textual representations of the environments, such as HTML and accessibility trees, which often require system-level permissions and are often lengthy, noisy, limited scalability [6, 64]. An appealing and promising direction is using Multimodal Large language models (MLLMs) to develop GUI agents capable of performing complex tasks

[†]Corresponding authors

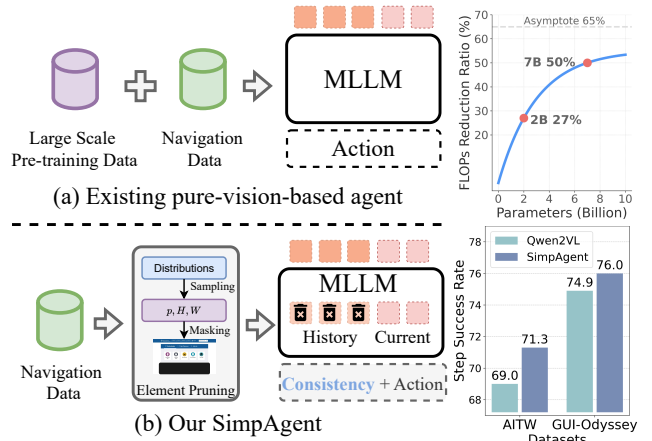


Figure 1. Compared to the large-scale pre-training scheme, we investigate the contextual modeling and propose an efficient training framework with element and history context simplification and additional consistency guidance. The resulting SimpAgent can achieve superior performance with 27% FLOPs reduction.

simply by analyzing the screenshots [11, 46, 54, 56]. These pure-vision-based GUI agents are implemented through either modular agent frameworks [11, 45, 46, 55] or end-to-end agent models [6, 56, 62]. Due to the significant gap between natural images and GUI screenshots, current pure-vision-based GUI agents primarily pursue comprehensive, high-quality pre-training data for improving GUI comprehension ability, which is very valuable but not computation-friendly, as shown in Figure 1.

Despite their advancements, building a powerful GUI agent still suffers from significant challenges related to contextual modeling. We analyze the characteristics of element and history contexts to uncover the underlying challenges. **1) The high-density and loose-relation of element context.** The statistical results in Figure 2 indicate that the number of elements per screenshot can reach dozens or even hundreds. These elements are not tightly integrated [28], unrelated elements may inadvertently affect each other’s functionality or appearance, hindering the comprehension of critical elements, empirically verified in Table 1. **2) The**

high redundancy of history context. Introducing historical observations will increase the computational overhead by 3.4 times, but only improve the performance by 3.0%, as shown in Table 1. The significant gap between computation and performance increments demonstrates a high redundancy in historical information, raising questions about the optimal utilization of historical information.

To address these challenges, we devise a **context-aware simplification framework** to construct an effective and efficient GUI Agent, termed **SimpAgent**. The main components within our framework are masking-based element pruning and consistency-guided history compression, enabling the efficient modeling of element and history contexts respectively, depicted in Figure 1. As unrelated elements obstruct the understanding of critical elements, the most effective solution is to eliminate them. By avoiding the challenges of intractable relationship modeling for pruning elements, we successfully reach this goal with an efficient masking mechanism. During the training phase, our **masking-based element pruning** method randomly masks a rectangular region based on a predefined distribution in the current screenshot. Because unrelated elements occupy a considerable portion of the screenshot, our masking operation can prune them with a high probability. We empirically observe a notable performance improvement even when the masked region reaches half of the screenshot.

To reduce the redundant historical visual information, we devise a **consistency-guided history compression** method with a token dropping strategy and a consistency guidance. Specifically, we first directly drop historical vision tokens at one specific LLM layer k , which will implicitly force LLM to compress historical visual information into preserved tokens. Our dropping strategy shares a similar finding with recent approaches [4, 13, 53], the shallow LLM layers can aggregate the vision features into a few anchor tokens (primarily adjacent action tokens in our cases). Compared to existing compression works [20, 27, 53, 59], our directly dropping strategy requires no extra parameters and enables efficient attention computation. Despite the significant efficiency of dropping, it still encounters the information loss caused by its implicit compression mechanism. Instead of reducing the dropping rate [4, 13] or adjusting the attention mask [59], we innovatively propose a consistency guidance to explicitly steer the compression. We additionally keep an original branch with unchanged tokens after layer k , and minimize the Kullback-Leibler divergence between the action predictions from two branches. The experiments indicate that our compression approach achieves a better trade-off between performance and computational efficiency.

We conduct comprehensive experiments on four representative GUI navigation datasets, AITW [37], Mind2Web [9], GUI-Odyssey [29], AndroidControl [18], to verify the effectiveness and computational efficiency of our methods.

The resulting SimpAgent can reduce the inference FLOPs by 27% and achieves significant performance gains of 2.3% and 1.1% on AITW and GUI-Odyssey, respectively. On the AndroidControl dataset, our SimpAgent improves the performance by 0.7% without any extra pre-training data. In contrast, OS-Altas achieves a performance gain of 0.8% with 1.9M pre-training GUI data.

Our contributions are summarized as follows:

1. We systematically analyze the UI screenshot and GUI Agent from the perspective of contextual modeling, and conclude the characteristics of element and history contexts, highlighting the underlying challenges overlooked in early works.
2. We propose a context-aware simplification framework with two novel components, masking-based element pruning and consistency-guided history compression, resulting in SimpAgent to efficiently and effectively extract essential elements and historical information.
3. Comprehensive experiments on four representative GUI navigation datasets, AITW [37], Mind2Web [9], GUI-Odyssey [29], AndroidControl [18], verify the effectiveness and computational efficiency of our SimpAgent.

2. Related works

GUI Agents. Autonomous agents powered [6, 16, 23, 24, 49, 57, 63] by (M)LLMs [3, 17, 19, 26, 42], have attracted considerable attention owing to their advanced interactive capabilities. Recent efforts have begun to enable agents to interact with web, mobile, and desktop operating systems, resulting in GUI agents [31, 48]. However, early works built agents [9, 35, 50, 60] via internal APIs or system backend codes, which is unavailable in most commercial software. This has prompted a shift in research focus toward pure-vision-based agents.

To leverage the understanding and reasoning capabilities of advanced foundation models (e.g., GPT-4o [15] and Gemini [44]), many works [11, 46, 52] attempt to build compositional, framework-based agents that generally contains multiple models (such as a Planner and an Actor). They collect or synthesize a large-scale GUI grounding corpus to develop strong foundation action models and combine them with an advanced Planner (based on GPT-4o or Gemini). Some works [36, 56] also curate lots of GUI navigation datasets to further build end-to-end native agents. Despite their advancements, the collection of such massive datasets requires substantial human and computational resources, which can have huge economic impacts.

Instead of massive data curation, a few works have attempted to construct effective and computation-friendly agents. OdysseyAgent [29] proposes a history resampler module to compress historical screenshots, but it overlooks the multi-modal interaction and introduces extra parameters compared to our method. Iris [10] and ShowUI [25]

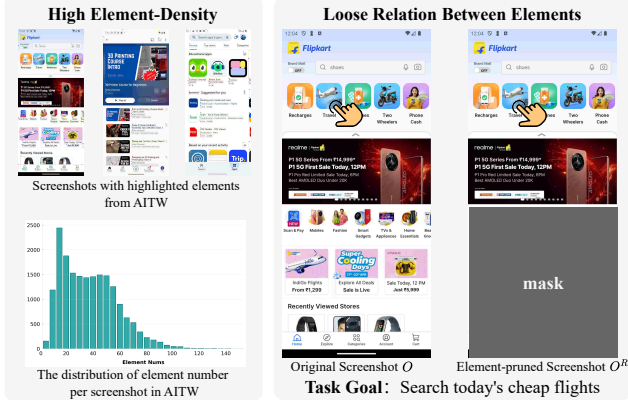


Figure 2. The illustration of high density and loose relation of elements in UI screenshots.

try to eliminate the useless background by leveraging low-level visual clues in UI screenshots, but they struggle to handle element-density screenshots. In contrast, we devise an efficient masking-based element-pruning method to enhance the comprehension of critical elements even in high element-density scenarios.

Vision Compression in MLLM. In the real world, multimodal content understanding plays a crucial role and holds significant value [39–41, 43]. This capability has been further enhanced and emphasized in multimodal large language models. As the number or resolution of images increases, the vision tokens in MLLMs will take up a significant portion of the limited context window and incur huge computational costs. To address it, previous works [8, 14, 17, 20, 61] mainly rely on a set of learnable queries to compress vision tokens, which requires a multi-stage dedicated training procedure. Some works [21, 27, 38] try to use token similarity to select vision tokens, but still introduce extra learnable parameters. Recently, FastV [4] has found that shallow LLM layers can aggregate visual features to some anchor tokens. VoCo-LLaMA [59] adjusts the attention masking to explicitly compress visual information into VoCo tokens, preventing efficient attention implementation (like FlashAttention). Victor [53] keeps the attention masking unchanged and implicitly summarizes visual information into some registers. In contrast to them, we propose direct token dropping and consistency guidance to achieve a better trade-off between performance and efficiency.

3. Preliminary

3.1. Problem Definition

GUI Agents, which are constructed for GUI Navigation tasks, can sequentially generate actions and interact with the GUI environment to achieve a task goal [31]. The interaction between an agent and the environment can be treated as a sequential decision-making process [48]. At time step t , the agent receives a task goal G , a history context H_t , a screenshot observation o_t , and then generates an action

Settings	#Tokens	FLOPs(T) (All / LLM)	Step SR
O	327	2.45 / 0.88	62.5
$O + 4A$	408	2.70 / 1.09	66.0
$O^R + 4A$	408	2.70 / 1.09	68.8
$O + 4AO$	1551	11.90 / 4.12	69.0

Table 1. The pilot experiments of GUI Agent on the AITW dataset. The base model is Qwen2-VL-2B. “ O ” (“ O^R ”) means only using current observation (pruned unrelated elements) to make a decision, while “ $+4AO$ ” or “ $+4A$ ” denotes additional adding 4 previous observation-actions or actions.

a_t . The history context contains previous screenshot observations and actions, $H_t = \{o_{t-\tau}, a_{t-\tau}, \dots, o_{t-1}, a_{t-1}\}$, where τ is history length, providing valuable multimodal information about the task completion status. If we represent the agent model as π_θ , the training objective of the agent can be formulated as follows:

$$\mathcal{L}(\pi_\theta) = - \sum_{t=0}^T \log \pi_\theta(a_t | o_t, H_t, G). \quad (1)$$

3.2. The high-density and loose-relation of element context

Perceiving the GUI screenshots is critical and challenging for the agent’s decision-making, due to the high element-density, intricate layout, and diverse styles of the interface [6, 54]. Figure 2 shows some screenshots on the mobile device, providing an intuitive representation of high-element density in the GUI scenario. Statistical analyses reveal that each screenshot in the AITW dataset [37] contains an average of 56 elements, while the AndroidControl dataset [18] has an average of 180 elements per screenshot.

Another distinctive characteristic of graphical elements is their loose relations. The associations between elements are often loose and changing, replacing, or hiding one element may not significantly impact the user’s ability to interact with or understand other elements. The main reason for these loose relations is the modular interface design principle, where components are designed to function independently [28]. In Figure 2, we present a case that masking bottom regions (including unrelated elements) in a screenshot has no impact on the decision-making compared to the usage of the original screenshot.

To further validate the loose relation between elements, we conduct a preliminary experiment by roughly splitting a screenshot observation O into two sets, the areas with related elements O^R and unrelated elements O^U . As each observation corresponds to an action (mostly a click operation), we assume that the areas far from the click point contain unrelated elements. Therefore, we consider half of the image containing the click point as O^R , and the rest is O^U . Table 1 show the decision-making performance (68.8%) on O^R is superior to that (66.0%) on O . The comparison con-

firm the existence of unrelated elements and highlights the potential interference they may cause.

3.3. The high redundancy of history context

The integration of historical information, including previous observations and actions, can help the agent to comprehend the completion status of the current task. As many GUI navigation tasks are quite complex and require a lot of steps to complete, effectively using history context is very valuable [29, 62]. Previous works [30, 62] mainly leverage the prior actions, which leads to considerable gains and a few extra tokens (generally 10-20 tokens per action). However, the vision information from previous observations is also important because the task progress can be accurately determined only with the combination of previous observations and actions [25].

Here, we present some pilot experiments of history observations and actions by fine-tuning Qwen2-VL-2B [47] as an agent on the popular GUI navigation task, AITW [37]. In Table 1, we compare the agent’s performance with different levels of history context, without history, with 4 previous actions, and with 4 previous actions and observations. It is clear that current observation has a dominant impact on the final outcome, only using current observation achieves 62.5% step success rate. Incorporating 4 actions can increase the step success rate by 3.5%, and further adding 4 observations leads to the gain of 3.0%. The current observation setting only requires 327 tokens, while the 4 observations additionally introduce 1143 tokens and increase the computational overhead by 3.4 times. The comparison of performance and computational increments indicates a significant redundancy in historical observation information, which can notably impact the agent’s inference speed and hinder its practical application.

4. A context-aware simplification framework

In this section, we will introduce our context-aware simplification framework with two novel methods, masking-based element pruning and consistency-guided history compression, as shown in Figure 3.

4.1. Masking-based Element Pruning

As analyzed above, the characteristic of high element-density in UI screenshots results in a significant challenge in perceiving valuable elements. To address it, current works [11, 54] mainly pursue the scaling of grounding pre-training data, which is effective but very expensive due to the cumbersome data collection process. In contrast, we adopt an orthogonal approach to elevate element comprehension capability in a data-efficient manner by leveraging the inherent characteristics of user interfaces (UIs). Our method is inspired by the implication of loose relations, that pruning some unrelated elements plausibly has no impact on the

comprehension of key elements. However, identifying what elements to prune is intractable cause the relation between elements is dependent on numerous factors, highly unpredictable [28]. To avoid the modeling of element relation, we devise a conceptually simple but effective method to prune elements by masking.

Our masking-based element pruning method selects a rectangle region \mathcal{R} in current observation o_t , and performs a masking operation \mathcal{M} on it. Assume the size of the selected region is $h \times w$, we randomly sample the size from a uniform distribution $U(a, b)$ where a, b are left and right bounds. The center point of the selected region is $p_c = (x_c, y_c)$, we randomly sample this point from a specific distribution (Gaussian or Uniform distribution). The masking operation will set the pixels within \mathcal{R} to a specific value v . The masking method and examples are represented in Figure 3. In training, our masking operation is conducted with a certain probability p . At inference, the masking operation is omitted to provide complete visual information.

$$o_t^m = \mathcal{M}(o_t) = \begin{cases} v, & (x, y) \in \mathcal{R}; \\ o_t(x, y), & \text{otherwise.} \end{cases} \quad (2)$$

Our core design principle is that the masking of unrelated elements can facilitate the comprehension of valuable elements. Our method can prune unrelated elements with a high probability for two reasons. 1) The most valuable elements cover a small area in the screenshot. we have conducted a statistical analysis and found that the average portion of click regions in the screenshot is 2%. 2) The loose relation between elements implies that unrelated elements occupy a considerable portion of the screenshot. These two reasons collectively ensure that the masking operation will not yield a large quantity of noise samples. In the experiment section, we find that notable performance improvements can still be achieved even when the masked region reaches half of the screenshot.

4.2. Consistency-guided History Compression

The high redundancy of history context requires us to compress the historical information and improve the inference efficiency of the agent. In comparison with few computation cost caused by the history actions, history observations additionally increase the computational overhead by 3.4 times. Thus, we focus on the compression of history visual information. Current vision compression approaches [20, 27, 58] mainly employ the extra-module-based paradigm, which will induce additional computational cost and hardly take into account the interaction between multiple modalities. Recently, some researchers [4, 13, 53] investigate the attention distribution of various types of tokens in a trained MLLM. They found that the shallow layers in LLM can aggregate the vision features into a few anchor tokens and the attention scores can be

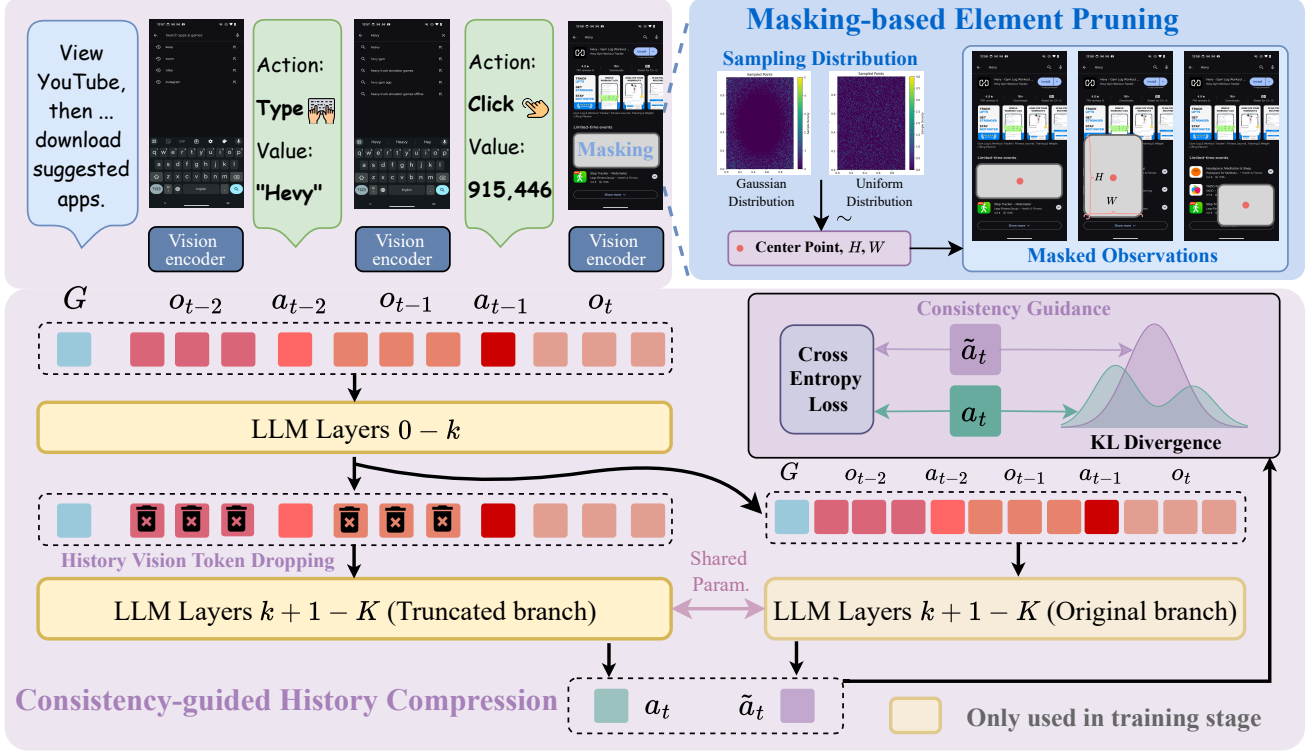


Figure 3. Overview of our context-aware simplification framework for building SimpAgent. The main components are masking-based element pruning and consistency-guided history compression. We assist SimpAgent in mitigating interference from unrelated elements by masking certain regions based on a pre-defined distribution. During training, we maintain the consistency between two LLM branches for explicitly steering history compression. At inference, SimpAgent only uses the LLM branch with truncated tokens, reducing 27% FLOPs.

used to identify these anchor tokens. These works can only retain the anchor tokens to accelerate the inference of a trained MLLM, but inevitably encounter performance degradation. In contrast, we propose a consistency-guided history compression method and apply it in the training stage to achieve a better trade-off between performance and computational efficiency.

Our consistency-guided history compression contains two key components, LLM-based history dropping and consistency-guided training objective. The history compression is internally processed within the LLM through the selective removal of vision tokens. After projecting task goal, raw observations, and actions to vision and text tokens, the concatenated token sequence $\{G, o_{t-\tau}, a_{t-\tau}, \dots, o_{t-1}, a_{t-1}, o_t\}$ is fed into a LLM to generate next action tokens a_t . We simply drop all history vision tokens $\{o_{t-\tau}, \dots, o_{t-1}\}$ after LLM layer k , and the LLM continues with the truncated token sequence $\{G, a_{t-\tau}, \dots, a_{t-1}, o_t\}$. The whole process is depicted in H_t^c

Figure 3. For simplicity, we represent the agent model with LLM-based history dropping as $\pi_\theta(a_t|o_t^m, H_t^c, G)$. The rationale behind this approach is that shallow layers in LLM

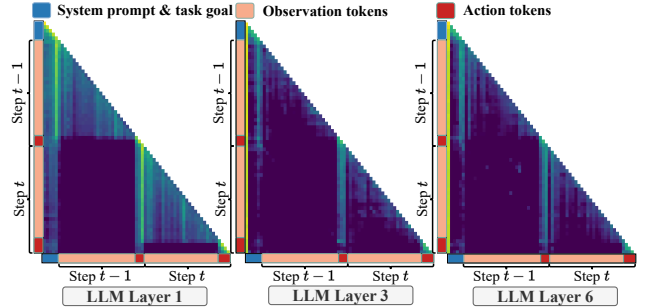


Figure 4. The attention maps during the LLM decoding process of GUI Agent. One previous step is used. We can see that in the shallow layers, attention distributes smoothly across various types of tokens within each step. In the deep layers, the attention scores within each step are aggregated to adjacent action tokens and attention over observation tokens is rather sparse.

can use causal self-attention to compress vision tokens into adjacent text tokens, which is also observed in Figure 4.

We find that the directly dropping strategy implicitly compresses the visual information through the causal self-attention mechanism, inevitably leading to some information loss. VoCo-LLaMA [59] introduces an explicit and strict compression method by adjusting the attention mask but suffers from severe computational efficiency issues. In contrast, we devise a consistency-guided training objective

to steer the vision compression process by maintaining the consistency between the truncated branch (with H_t^c) and the original branch (with H_t). The training objective is formulated as follows:

$$\begin{aligned} \mathcal{L}(\pi_\theta) = & -\mathbb{D}_{KL}[\pi_\theta(\tilde{a}_t|o_t^m, H_t, G) \parallel \pi_\theta(a_t|o_t^m, H_t^c, G)] \\ & - \sum_{t=0}^T \log \pi_\theta(\tilde{a}_t|o_t^m, H_t, G) - \sum_{t=0}^T \log \pi_\theta(a_t|o_t^m, H_t^c, G). \end{aligned} \quad (3)$$

5. Experiments

In this section, we validate our model using comprehensive agent benchmarks that cover various mobile scenarios. We use Qwen2VL-2B [47] as our base model and fine-tune it on GUI Navigation datasets to obtain our SimpAgent. The implementation details can be found in section B in Appendix.

5.1. Datasets

We select four GUI navigation datasets, to evaluate SimpAgent’s multi-step execution ability. Table 2 shows the statistical analysis of these datasets.

Dataset	Domain	#Task	#Avg. Steps
AITW [37]	Mobile & Web	2,939	8.1
Mind2Web [9]	Web	2,350	7.3
GUI-Odyssey [29]	Mobile	7,735	15.4
AndroidControl [18]	Mobile	15,283	5.5

Table 2. Dataset statistics, including domain, number of tasks, and average task length (measured in steps).

5.2. Main Results

In Tables 3, we present the evaluation results of our SimpAgent on mobile and web navigation datasets, AITW, Mind2Web, GUI-Odyssey. In comparison with SeeClick [6], Iris [10], and ShowUI [25], our agent demonstrated superior performance without pre-training GUI datasets and fewer or comparable parameters. We also evaluate our SimpAgent on a long-horizon navigation dataset, GUI-Odyssey with average steps of 15.4. In the last column of Table 3, we find that SimpAgent outperforms OdysseyAgent [29] with fewer parameters, suggesting its superior capability of history information utilization. In Table 4, we evaluate our model on the most diverse mobile navigation dataset, AndroidControl, with 833 Android apps. We adopt the setting of only using high-level instructions. Notably, with no extra pre-training data and smaller model size, SimpAgent-2B yields comparable performance gain (increase 0.7% over the baseline Qwen2VL) with OS-Atlas4B [54] (increase 0.8% over the baseline InternVL2) which has been pre-trained on large-scale GUI datasets (1.9M). These comparisons suggest that our context-aware simplification framework can assist agents in effectively extracting

critical elements and enhancing the agent’s navigation capability. We also evaluate our SimpAgent and its variants on the Mind2Web dataset with three challenging out-of-the-domain testing sets, obtaining new state-of-the-art performances. **More detailed comparisons can be found in Table 1-3 in Appendix.**

5.3. Ablation Studies

Ablation of all components. In Table 5, we examine all components in our context-aware simplification framework. The comparisons begin with history compression, followed by the addition of consistency guidance, and conclude with masking-based element pruning. As shown, if historical screenshots are compressed by directly dropping, the information loss is significant (decreases 1.7% and 3.1% on AITW and GUI-Odyssey respectively) due to the implicit supervision mechanism. However, the compression results in a significant inference acceleration and achieves 27% FLOPs reduction. By utilizing consistency loss to explicitly steer the process with complete historical information, the compression of historical visual information can be significantly enhanced, achieving nearly lossless results (a gap of 0.1%) on AITW and competitive performance (a gap of 1.2%) on GUI-Odyssey. The masking-based element pruning method further enhances performance by filtering out irrelevant element noise during the learning process, leading to superior results (increase 2.4% and 2.3% on AITW and GUI-Odyssey separately). This demonstrates the effectiveness of our proposed masking-based element pruning and consistency-guided history compression methods.

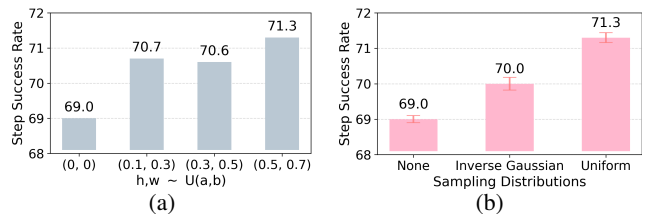


Figure 5. (a): The analysis of masking region $(h, w \sim U(a, b))$ in masking-based element pruning module. (b): The analysis of masking strategy based on different sampling distributions.

The analysis of masking region choice. In Figure 5 (a), we analyze the selection of parameters for the size of mask region, where both h and w are independently sampled from $U(a, b)$. We fix the masking probability to 0.5 and sample the center point p_c from a uniform distribution. Under different settings of the a, b parameters, our method consistently improves without significant performance fluctuations, proving the effectiveness and insensitivity of the approach. When parameters a and b are selected from the range (0.5, 0.7), the corresponding mask will cover 25% to 50% of the image region. Even with such a large masked area, it still effectively enhances the model’s learning, indicating that unrelated elements occupy a significant portion

Method	#P.T.	#Param.	AITW	Mind2Web			GUI-Odyssey
				Cross-Task	Cross-Website	Cross-Domain	
CogAgent [12]	140M	18B	-	17.6	13.4	15.5	11.84
Qwen-VL [1]	-	9.6B	54.3	13.3	9.2	12.0	72.8
SeeClick [6]	850K	9.6B	59.3	25.5	16.4	20.8	-
OdysseyAgent [29]	-	9.6B	-	-	-	-	74.3
Qwen2VL* [47]	-	2B	66.0	45.0	40.9	40.5	69.0
Qwen2VL [47]	-	2B	69.0	46.7	42.2	44.6	74.9
Iris [10]	850K	9.6B	63.6	32.0	26.2	28.8	-
ShowUI [25]	256K	2B	70.0	37.2	35.1	35.2	-
SimpAgent	-	2B	71.3	47.1	42.8	43.3	76.0
SimpAgent-M	-	2B	71.5	48.7	42.2	45.0	77.4

Table 3. Performance comparisons on AITW, Mind2Web, and GUI-Odyssey. We report the step success rate (step SR). “#P.T.”, and “#Param.” denote the number of pre-training GUI datasets and parameters, respectively. “*” means the variant utilizing only action history. “-M” denotes only applying masking-based element pruning without inference FLOPs reduction.

Method	#P.T.	#Param.	AndroidControl-High		
			Type	Grounding	SR
SeeClick [6]	850K	9.6B	82.9	62.9	59.1
InternVL2 [5]	-	4B	84.1	72.7	66.7
OS-Atlas [54]	1.9M	4B	84.7	73.8	67.5
Qwen2VL* [47]	-	2B	84.4	72.2	67.8
Qwen2VL [47]	-	2B	84.5	72.9	68.4
SimpAgent	-	2B	84.9	73.2	69.1
SimpAgent-M	-	2B	84.8	73.8	69.3

Table 4. Main Results on Android Control. “#P.T.”, “#Param.” and “SR” denote the number of pre-training GUI datasets and parameters, and step success rate, respectively. “*” means the variant utilizing only action history. “-M” denotes only applying masking-based element pruning without inference FLOPs reduction.

C.p.	C. C.p.	M. P.	FLOPs	AITW	GUI-Odyssey
			11.90	69.0	74.9
✓			8.71 \downarrow 27%	67.3 \downarrow 1.7	71.8 \downarrow 3.1
✓	✓		8.71 \downarrow 0%	68.9 \uparrow 1.6	73.7 \uparrow 1.9
✓	✓	✓	8.71 \downarrow 0%	71.3\uparrow2.4	76.0\uparrow2.3

Table 5. Ablation study of all components in our context-aware simplification framework. “C.p.” and “C. C.p.” mean history compression and consistency-guided history compression. “M. P.” denotes masking-based element pruning.

of the screenshot.

The analysis of different masking distributions. In Figure 5 (b), we analyze the impact of using uniform and inverse gaussian distributions for sampling the center point of masking regions. We set the masking probability $p = 0.5$ and the size $h, w \sim U(0.5, 0.7)$. The design of the Inverse Gaussian distribution is based on an intuitive prior: elements closer to the current operation point are more relevant to the task and should be masked with a smaller probability. Inverse Gaussian distribution achieves a performance improvement of 1% compared to the non-mask variants, but it still underperforms the Uniform distribution. Notably, we also report the standard deviations, which are no more than 0.2%, indicating the robustness of our masking strategy. Experimental results suggest that the element distribution

is more complex than initially assumed. This could be due to the intricate relationships between different elements in the GUI design, where the applications have highly diverse operational logic and layouts [28]. Therefore, adopting a uniform distribution could be a solid choice, but a better solution remains to be explored.

The analysis of drop layer choice. In Table 6 we analyze the selection of the drop layer k in LLM. It is shown that the shallow layers indeed realize a certain level of information transfer, as $k = 1$ has a better performance of 66.5% than the setting of utilizing only action history (66.0%). After $k = 3$, the step success rate reaches a saturation point (around 67.3%) with the minimal performance degradation. This phenomenon is also observed in recent studies [4, 53] on general multimodal comprehension tasks, confirming the generalization of the token compression mechanism within LLM layers across various scenarios.

5.4. Comparison with other compression methods

The existing compression schemes are divided into extra-module-based [20, 27] and LLM-based compression methods [4, 13, 53, 59]. For the extra-module-based approach, we select the Token Merger [27] as a representative work. It uses a token filter algorithm to select the most valuable tokens, utilizing these tokens as queries and employing cross-attention to further aggregate all the features. For the LLM-based compression method, we select Victor [53] and FastV [4]. These two methods both use summary tokens to compress visual information, but the former is applied in the training stage and the summary tokens are trainable to aggregate information, the latter focuses on inference acceleration by selecting the most valuable vision tokens as summary tokens based on attention scores.

For a fair comparison, we fix the number of selected (Token Merger) or summary (Victor and FastV) tokens at 64, and adopt the setting of Qwen2VL with 4 history screenshots and actions. The Token Merger utilizes the resampler module to compress each historical image into 64 tokens.

k	1	3	6	12
Step SR	66.5	67.3	66.8	67.4
FLOPs (T)	8.49 \downarrow 29%	8.71 \downarrow 27%	9.03 \downarrow 24%	9.67 \downarrow 19%

Table 6. The analysis of drop layer k in history compression module without consistency guidance. The uncompressed FLOPs and performance are 11.9 and 69.0.



Figure 6. Illustration of some navigation steps successfully predicted by our SimpAgent, while incorrectly predicted by the baseline Qwen2-VL. The attention maps of final action tokens corresponding to the observations confirm SimpAgent can identify correct elements among distracting elements.

Victor introduces τ groups of 64 summary tokens for τ history screenshots. After the third layer, only the summary tokens are retained and the historical vision tokens are discarded. FastV is applied to the trained Qwen2VL model, where “-0” means 0% of the historical vision tokens are selected as summary tokens during inference. “-50” denotes 50% of the historical vision tokens are selected.

As shown in Table 7, compared to training-based methods, Token Merger and FastV, our approach has lower FLOPs and smaller performance loss, owing to the intrinsic compression mechanism of LLM and the explicit consistency constraint. In contrast, Token Merger requires the introduction of additional parameter modules, while Victor suffers from poor performance due to the lack of explicit guidance for the compression process. As an inference-only method, FastV fails to learn better compressed features. Compared to FastV-0, our approach outperforms it by 5.1% in the step success rate metric at the same computational complexity. While FastV-50 achieves slight improvements by retaining more vision tokens, its efficiency and performance still fall short compared to our method. These comparisons demonstrate that our consistency-guided compression method can reach an optimal balance between performance and computational efficiency.

5.5. Qualitative Analysis

To enhance the understanding of our SimpAgent, we investigate the change of attention distribution after applying the proposed masking-based element pruning and consistency guidance. Figure 6 illustrates some navigation steps that are successfully executed by our SimpAgent, while the baseline model (fine-tuned Qwen2VL) fails to complete these steps.

Method	No	Token Merger	Victor	FastV-50	FastV-0	Ours
Step SR	69.0	68.9	67.6	66.0	63.8	68.9
FLOPs (T)	11.90	9.28	9.28	10.15	8.71	8.71

Table 7. Comparison to other extra-module-based (TokenMerger [27]) and LLM-based (Victor[53], FastV[4]) compression methods.

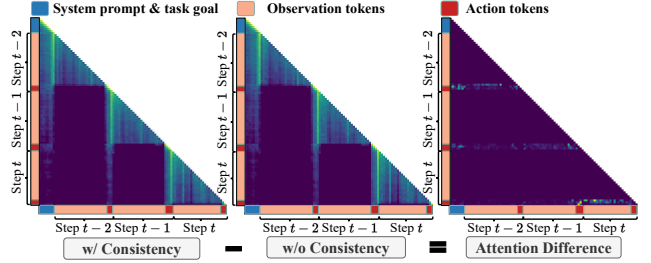


Figure 7. Illustration of attention maps in agent models w/ and w/o consistency guidance, and their attention difference map. The **attention difference map** shows that action tokens pay more attention (highlighted positions) to historical observation tokens when they act as query tokens with consistency guidance. This attention comparison demonstrates that consistency guidance can promote the information aggregation from observations to actions and facilitate the history compression.

We present the attention maps of generated action tokens associated with the current screenshot, averaged across tokens and all attention heads. These visualizations demonstrate that our SimpAgent can attend to the valuable elements (indicated by the peak of attention), as the masking strategy mitigates interference from unrelated elements.

We also analyze the information flow in the agent models with and without consistency guidance. Figure 7 shows the attention maps of all tokens when the agent is trained with and without consistency guidance. To investigate the information flow of historical observations and actions, we present the attention difference map by subtracting the map without guidance from the map with consistency guidance. Note that the resulting map only highlights the difference in attention scores of action tokens to other tokens for clear comparisons. The difference map suggests that the historical action tokens pay more attention to the adjacent historical vision tokens under the setting of consistency guidance. This attention enhancement provides a clear explanation of the underlying working mechanism of the proposed consistency constraint, revealing the better information aggregation caused by this explicit supervision.

6. Conclusion

We introduced SimpAgent, an MLLM-based autonomous agent for GUI navigation. For building it, we devise a context-aware simplification training framework to facilitate comprehensive cognition with accurate element perception and efficient history modeling. SimpAgent is enhanced with two key components, masking-based element pruning

and consistency-guided history compression. The former mitigate the interference from unrelated elements and improve the understanding of critical elements for enhanced navigation. The latter reduces the computational cost of history vision modeling, and adds the consistency guidance for better balance between performance and efficiency. SimpAgent achieves state-of-the-art performances on diverse GUI benchmarks with fewer parameters and no GUI data pre-training. These comparisons highlight SimpAgent’s potential to promote the development of future GUI agents.

References

- [1] Jinze Bai, Shuai Bai, Shusheng Yang, Shijie Wang, Sinan Tan, Peng Wang, Junyang Lin, Chang Zhou, and Jingren Zhou. Qwen-VL: A Frontier Large Vision-Language Model with Versatile Abilities. *arXiv preprint*, 2023. 7, 14
- [2] Hyungjoo Chae, Namyoung Kim, Kai Tzu-iunn Ong, Minju Gwak, Gwanwoo Song, Jihoon Kim, Sunghwan Kim, Dongha Lee, and Jinyoung Yeo. Web Agents with World Models: Learning and Leveraging Environment Dynamics in Web Navigation. In *The Thirteenth International Conference on Learning Representations, 2024*. arXiv, 2024. 1
- [3] Gongwei Chen, Leyang Shen, Rui Shao, Xiang Deng, and Liqiang Nie. Lion: Empowering multimodal large language model with dual-level visual knowledge. In *Proceedings of the IEEE/CVF Conference on Computer Vision and Pattern Recognition*, pages 26540–26550, 2024. 2
- [4] Liang Chen, Haozhe Zhao, Tianyu Liu, Shuai Bai, Junyang Lin, Chang Zhou, and Baobao Chang. An Image is Worth 1/2 Tokens After Layer 2: Plug-and-Play Inference Acceleration for Large Vision-Language Models. In *European Conference on Computer Vision, 2024*. arXiv, 2024. 2, 3, 4, 7, 8
- [5] Zhe Chen, Jiannan Wu, Wenhai Wang, Weijie Su, Guo Chen, Sen Xing, Muyan Zhong, Qinglong Zhang, Xizhou Zhu, Lewei Lu, Bin Li, Ping Luo, Tong Lu, Yu Qiao, and Jifeng Dai. InternVL: Scaling up Vision Foundation Models and Aligning for Generic Visual-Linguistic Tasks. *arXiv preprint*, 2023. 7
- [6] Kanzhi Cheng, Qiushi Sun, Yougang Chu, Fangzhi Xu, Yantao Li, Jianbing Zhang, and Zhiyong Wu. SeeClick: Harnessing GUI Grounding for Advanced Visual GUI Agents. In *Proceedings of the 62nd Annual Meeting of the Association for Computational Linguistics*. arXiv, 2024. 1, 2, 3, 6, 7, 12, 14
- [7] Filippos Christianos, Georgios Papoudakis, Matthieu Zimmer, Thomas Coste, Zhihao Wu, Jingxuan Chen, Khyati Khandelwal, James Doran, Xidong Feng, Jiacheng Liu, Zheng Xiong, Yicheng Luo, Jianye Hao, Kun Shao, Haitham Bou-Ammar, and Jun Wang. Pangu-Agent: A Fine-Tunable Generalist Agent with Structured Reasoning. *arXiv preprint*, 2023. 1
- [8] Wenliang Dai, Junnan Li, Dongxu Li, Anthony Meng Huat Tiong, Junqi Zhao, Weisheng Wang, Boyang Li, Pascale Fung, and Steven Hoi. InstructBLIP: Towards General-purpose Vision-Language Models with Instruction Tuning. *arXiv preprint*, 2023. 3
- [9] Xiang Deng, Yu Gu, Boyuan Zheng, Shijie Chen, Samuel Stevens, Boshi Wang, Huan Sun, and Yu Su. Mind2Web: Towards a Generalist Agent for the Web. In *Advances in Neural Information Processing Systems, 2023*. arXiv, 2023. 2, 6, 12
- [10] Zhiqi Ge, Juncheng Li, Xinglei Pang, Minghe Gao, Kaihang Pan, Wang Lin, Hao Fei, Wenqiao Zhang, Siliang Tang, and Yueting Zhuang. Iris: Breaking GUI Complexity with Adaptive Focus and Self-Refining. *arXiv preprint*, 2024. 2, 6, 7, 14
- [11] Boyu Gou, Ruohan Wang, Boyuan Zheng, Yanan Xie, Cheng Chang, Yiheng Shu, Huan Sun, and Yu Su. Navigating the Digital World as Humans Do: Universal Visual Grounding for GUI Agents. *arXiv preprint*, 2024. 1, 2, 4
- [12] Wenyi Hong, Weihang Wang, Qingsong Lv, Jiazheng Xu, Wenmeng Yu, Junhui Ji, Yan Wang, Zihan Wang, Yuxuan Zhang, Juanzi Li, Bin Xu, Yuxiao Dong, Ming Ding, and Jie Tang. CogAgent: A Visual Language Model for GUI Agents. In *IEEE/CVF Conference on Computer Vision and Pattern Recognition*. arXiv, 2023. 7, 14
- [13] Lianyu Hu, Fanhua Shang, Liang Wan, and Wei Feng. iLLaVA: An Image is Worth Fewer Than 1/3 Input Tokens in Large Multimodal Models. *arXiv preprint*, 2024. 2, 4, 7
- [14] Wenbo Hu, Yifan Xu, Yi Li, Weiye Li, Zeyuan Chen, and Zhuowen Tu. BLIVA: A Simple Multimodal LLM for Better Handling of Text-Rich Visual Questions. *arXiv preprint*, 2023. 3
- [15] Aaron Hurst, Adam Lerer, Adam P Goucher, Adam Perelman, Aditya Ramesh, Aidan Clark, AJ Ostrow, Akila Welihinda, Alan Hayes, Alec Radford, et al. Gpt-4o system card. *arXiv preprint*, 2024. 2, 14
- [16] Hao Li, Qi Lv, Rui Shao, Xiang Deng, Yinchuan Li, Jianye Hao, and Liqiang Nie. Star: Learning diverse robot skill abstractions through rotation-augmented vector quantization. *International Conference on Machine Learning*, 2025. 2
- [17] Junnan Li, Dongxu Li, Silvio Savarese, and Steven Hoi. BLIP-2: Bootstrapping Language-Image Pre-training with Frozen Image Encoders and Large Language Models. In *International Conference on Machine Learning*. arXiv, 2023. 2, 3
- [18] Wei Li, William Bishop, Alice Li, Chris Rawles, Folawiyo Campbell-Ajala, Divya Tyamagundlu, and Oriana Riva. On the Effects of Data Scale on Computer Control Agents. In *Advances in Neural Information Processing Systems*. arXiv, 2024. 2, 3, 6, 12
- [19] Wei Li, Bing Hu, Rui Shao, Leyang Shen, and Liqiang Nie. Lion-fs: Fast & slow video-language thinker as online video assistant. In *Proceedings of the Computer Vision and Pattern Recognition Conference*, pages 3240–3251, 2025. 2
- [20] Yanwei Li, Chengyao Wang, and Jiaya Jia. LLaMA-VID: An Image is Worth 2 Tokens in Large Language Models. In *European Conference on Computer Vision, 2024*. arXiv, 2023. 2, 3, 4, 7
- [21] Yanwei Li, Yuechen Zhang, Chengyao Wang, Zhisheng Zhong, Yixin Chen, Ruihang Chu, Shaoteng Liu, and Jiaya Jia. Mini-Gemini: Mining the Potential of Multi-modality Vision Language Models. *arXiv preprint*, 2024. 3

- [22] Yinchuan Li, Xinyu Shao, Jianping Zhang, Haozhi Wang, Leo Maxime Brunswic, Kaiwen Zhou, Jiqian Dong, Kaiyang Guo, Xiu Li, Zhitang Chen, et al. Generative models in decision making: A survey. *arXiv preprint*, 2025. 1
- [23] Zaijing Li, Yuquan Xie, Rui Shao, Gongwei Chen, Dongmei Jiang, and Liqiang Nie. Optimus-1: Hybrid multimodal memory empowered agents excel in long-horizon tasks. In *Advances in Neural Information Processing Systems*, pages 49881–49913, 2024. 2
- [24] Zaijing Li, Yuquan Xie, Rui Shao, Gongwei Chen, Dongmei Jiang, and Liqiang Nie. Optimus-2: Multimodal minecraft agent with goal-observation-action conditioned policy. In *Proceedings of the Computer Vision and Pattern Recognition Conference*, pages 9039–9049, 2025. 2
- [25] Kevin Qinghong Lin, Linjie Li, Difei Gao, Zhengyuan Yang, Shiwei Wu, Zechen Bai, Weixian Lei, Lijuan Wang, and Mike Zheng Shou. ShowUI: One Vision-Language-Action Model for GUI Visual Agent. In *IEEE/CVF Conference on Computer Vision and Pattern Recognition*, 2024. 2, 4, 6, 7, 14
- [26] Haotian Liu, Chunyuan Li, Qingyang Wu, and Yong Jae Lee. Visual Instruction Tuning, 2023. 2
- [27] Yuliang Liu, Biao Yang, Qiang Liu, Zhang Li, Zhiyin Ma, Shuo Zhang, and Xiang Bai. TextMonkey: An OCR-Free Large Multimodal Model for Understanding Document. *arXiv preprint*, 2024. 2, 3, 4, 7, 8
- [28] Jonas Löwgren. *Thoughtful Interaction Design: A Design Perspective on Information Technology*. MIT Press, Cambridge, Massachusetts, 2004. 1, 3, 4, 7
- [29] Quanfeng Lu, Wenqi Shao, Zitao Liu, Fanqing Meng, Boxuan Li, Botong Chen, Siyuan Huang, Kaipeng Zhang, Yu Qiao, and Ping Luo. GUI Odyssey: A Comprehensive Dataset for Cross-App GUI Navigation on Mobile Devices. *arXiv preprint*, 2024. 2, 4, 6, 7, 12, 14
- [30] Xinbei Ma, Zhuosheng Zhang, and Hai Zhao. CoCo-Agent: A Comprehensive Cognitive MLLM Agent for Smartphone GUI Automation. In *Findings of the Association for Computational Linguistics*. arXiv, 2024. 4
- [31] Dang Nguyen, Jian Chen, Yu Wang, Gang Wu, Namyong Park, Zhengmian Hu, Hanjia Lyu, Junda Wu, Ryan Aponte, Yu Xia, Xintong Li, Jing Shi, Hongjie Chen, Viet Dac Lai, Zhouhang Xie, Sungchul Kim, Ruiyi Zhang, Tong Yu, Mehrab Tanjim, Nesreen K. Ahmed, Puneet Mathur, Seunghyun Yoon, Lina Yao, Branislav Kveton, Thien Huu Nguyen, Trung Bui, Tianyi Zhou, Ryan A. Rossi, and Franck Dernoncourt. GUI Agents: A Survey. *arXiv preprint*, 2024. 2, 3
- [32] OpenAI. Gpt-4 technical report, 2023. 14
- [33] Ajay Patel, Markus Hofmarcher, Claudiu Leoveanu-Condrei, Marius-Constantin Dinu, Chris Callison-Burch, and Sepp Hochreiter. Large Language Models Can Self-Improve At Web Agent Tasks. *arXiv preprint*, 2024. 1
- [34] Pranav Putta, Edmund Mills, Naman Garg, Sumeet Motwani, Elan Markowitz, Chelsea Finn, and Rafael Rafailov. Agent Q: Advanced Reasoning and Learning for Autonomous AI Agents. *arXiv preprint*.
- [35] Zehan Qi, Xiao Liu, Iat Long Iong, Hanyu Lai, Xueqiao Sun, Xinyue Yang, Jiadai Sun, Yu Yang, Shuntian Yao, Tianjie Zhang, Wei Xu, Jie Tang, and Yuxiao Dong. WebRL: Training LLM Web Agents via Self-Evolving Online Curriculum Reinforcement Learning. *arXiv preprint*, 2024. 1, 2
- [36] Yujia Qin, Yining Ye, Junjie Fang, Haoming Wang, Shihao Liang, Shizuo Tian, Junda Zhang, Jiahao Li, Yunxin Li, Shijue Huang, Wanjun Zhong, Kuanye Li, Jiale Yang, Yu Miao, Woyu Lin, Longxiang Liu, Xu Jiang, Qianli Ma, Jingyu Li, Xiaojun Xiao, Kai Cai, Chuang Li, Yaowei Zheng, Chaolin Jin, Chen Li, Xiao Zhou, Minchao Wang, Haoli Chen, Zhaojian Li, Haihua Yang, Haifeng Liu, Feng Lin, Tao Peng, Xin Liu, and Guang Shi. UI-TARS: Pioneering Automated GUI Interaction with Native Agents. *arXiv preprint*, 2025. 2
- [37] Christopher Rawles, Alice Li, Daniel Rodriguez, Oriana Riva, and Timothy Lillicrap. Android in the Wild: A Large-Scale Dataset for Android Device Control. In *Advances in Neural Information Processing Systems, 2023*, 2023. 2, 3, 4, 6, 12
- [38] Yuzhang Shang, Mu Cai, Bingxin Xu, Yong Jae Lee, and Yan Yan. LLaVA-PruMerge: Adaptive Token Reduction for Efficient Large Multimodal Models. *arXiv preprint*, 2024. 3
- [39] Rui Shao, Xiangyuan Lan, Jiawei Li, and Pong C Yuen. Multi-adversarial discriminative deep domain generalization for face presentation attack detection. In *Proceedings of the IEEE/CVF conference on computer vision and pattern recognition*, pages 10023–10031, 2019. 3
- [40] Rui Shao, Tianxing Wu, and Ziwei Liu. Detecting and grounding multi-modal media manipulation. In *Proceedings of the IEEE/CVF Conference on Computer Vision and Pattern Recognition*, pages 6904–6913, 2023.
- [41] Rui Shao, Tianxing Wu, Jianlong Wu, Liqiang Nie, and Ziwei Liu. Detecting and grounding multi-modal media manipulation and beyond. *IEEE Transactions on Pattern Analysis and Machine Intelligence*, 2024. 3
- [42] Leyang Shen, Gongwei Chen, Rui Shao, Weili Guan, and Liqiang Nie. Mome: Mixture of multimodal experts for generalist multimodal large language models. In *Advances in Neural Information Processing Systems*, pages 42048–42070, 2024. 2
- [43] Aleksandar Shtedritski, Christian Rupprecht, and Andrea Vedaldi. What does CLIP know about a red circle? Visual prompt engineering for VLMs, 2023. 3
- [44] Gemini Team, Rohan Anil, Sebastian Borgeaud, Jean-Baptiste Alayrac, Jiahui Yu, Radu Soricut, Johan Schalkwyk, Andrew M Dai, Anja Hauth, Katie Millican, et al. Gemini: a family of highly capable multimodal models. *arXiv preprint*, 2023. 2
- [45] Junyang Wang, Haiyang Xu, Haitao Jia, Xi Zhang, Ming Yan, Weizhou Shen, Ji Zhang, Fei Huang, and Jitao Sang. Mobile-Agent-v2: Mobile Device Operation Assistant with Effective Navigation via Multi-Agent Collaboration. In *Advances in Neural Information Processing Systems*. arXiv, 2024. 1
- [46] Junyang Wang, Haiyang Xu, Jiabo Ye, Ming Yan, Weizhou Shen, Ji Zhang, Fei Huang, and Jitao Sang. Mobile-Agent: Autonomous Multi-Modal Mobile Device Agent with Visual Perception. *arXiv preprint*, 2024. 1, 2
- [47] Peng Wang, Shuai Bai, Sinan Tan, Shijie Wang, Zhihao Fan, Jinze Bai, Keqin Chen, Xuejing Liu, Jialin Wang, Wenbin

- Ge, Yang Fan, Kai Dang, Mengfei Du, Xuancheng Ren, Rui Men, Dayiheng Liu, Chang Zhou, Jingren Zhou, and Junyang Lin. Qwen2-VL: Enhancing Vision-Language Model’s Perception of the World at Any Resolution. *arXiv preprint*, 2024. 4, 6, 7, 14
- [48] Shuai Wang, Weiwen Liu, Jingxuan Chen, Weinan Gan, Xingshan Zeng, Shuai Yu, Xinlong Hao, Kun Shao, Yasheng Wang, and Ruiming Tang. GUI Agents with Foundation Models: A Comprehensive Survey. *arXiv preprint*, 2024. 2, 3
- [49] Zihao Wang, Shaofei Cai, Anji Liu, Yonggang Jin, Jinbing Hou, Bowei Zhang, Haowei Lin, Zhaofeng He, Zilong Zheng, Yaodong Yang, Xiaojian Ma, and Yitao Liang. JARVIS-1: Open-World Multi-task Agents with Memory-Augmented Multimodal Language Models, 2023. 2
- [50] Zora Zhiruo Wang, Jiayuan Mao, Daniel Fried, and Graham Neubig. Agent Workflow Memory. *arXiv preprint*, 2024. 2
- [51] Hao Wen, Yuanchun Li, Guohong Liu, Shanhuai Zhao, Tao Yu, Toby Jia-Jun Li, Shiqi Jiang, Yunhao Liu, Yaqin Zhang, and Yunxin Liu. AutoDroid: LLM-powered Task Automation in Android. In *Proceedings of the 30th Annual International Conference on Mobile Computing and Networking*. arXiv, 2024. 1
- [52] Hao Wen, Hongming Wang, Jiaxuan Liu, and Yuanchun Li. DroidBot-GPT: GPT-powered UI Automation for Android. *arXiv preprint*, 2024. 2
- [53] Yuxin Wen, Qingqing Cao, Qichen Fu, Sachin Mehta, and Mahyar Najibi. Efficient Vision-Language Models by Summarizing Visual Tokens into Compact Registers. *arXiv preprint*, 2024. 2, 3, 4, 7, 8
- [54] Zhiyong Wu, Zhenyu Wu, Fangzhi Xu, Yian Wang, Qiushi Sun, Chengyou Jia, Kanzhi Cheng, Zichen Ding, Liheng Chen, Paul Pu Liang, and Yu Qiao. OS-ATLAS: A Foundation Action Model for Generalist GUI Agents. *arXiv preprint*, 2024. 1, 3, 4, 6, 7, 12
- [55] Bin Xie, Rui Shao, Gongwei Chen, Kaiwen Zhou, Yinchuan Li, Jie Liu, Min Zhang, and Liqiang Nie. Gui-explorer: Autonomous exploration and mining of transition-aware knowledge for gui agent. *The 63rd Annual Meeting of the Association for Computational Linguistics*, 2025. 1
- [56] Yiheng Xu, Zekun Wang, Junli Wang, Dunjie Lu, Tianbao Xie, Amrita Saha, Doyen Sahoo, Tao Yu, and Caiming Xiong. Aguis: Unified Pure Vision Agents for Autonomous GUI Interaction. *arXiv preprint*, 2024. 1, 2
- [57] Shunyu Yao, Jeffrey Zhao, Dian Yu, Nan Du, Izhak Shafran, Karthik Narasimhan, and Yuan Cao. ReAct: Synergizing Reasoning and Acting in Language Models. <https://arxiv.org/abs/2210.03629v3>, 2022. 2
- [58] Qinghao Ye, Haiyang Xu, Jiabo Ye, Ming Yan, Anwen Hu, Haowei Liu, Qi Qian, Ji Zhang, Fei Huang, and Jingren Zhou. mPLUG-Owl2: Revolutionizing Multi-modal Large Language Model with Modality Collaboration, 2023. 4
- [59] Xubing Ye, Yukang Gan, Xiaoke Huang, Yixiao Ge, Ying Shan, and Yansong Tang. VoCo-LLaMA: Towards Vision Compression with Large Language Models. *arXiv preprint*, 2024. 2, 3, 5, 7
- [60] Chi Zhang, Zhao Yang, Jiaxuan Liu, Yucheng Han, Xin Chen, Zebiao Huang, Bin Fu, and Gang Yu. AppAgent: Multimodal Agents as Smartphone Users. *arXiv preprint*, 2023. 1, 2
- [61] Renshan Zhang, Rui Shao, Gongwei Chen, Miao Zhang, Kaiwen Zhou, Weili Guan, and Liqiang Nie. Falcon: Resolving visual redundancy and fragmentation in high-resolution multimodal large language models via visual registers. In *Proceedings of the IEEE/CVF International Conference on Computer Vision (ICCV)*, 2025. 3
- [62] Zhuosheng Zhang and Aston Zhang. You Only Look at Screens: Multimodal Chain-of-Action Agents. In *Findings of the Association for Computational Linguistics*. arXiv, 2024. 1, 4
- [63] Ziniu Zhang, Shulin Tian, Liangyu Chen, and Ziwei Liu. MMInA: Benchmarking Multihop Multimodal Internet Agents, 2024. 2
- [64] Boyuan Zheng, Boyu Gou, Jihyung Kil, Huan Sun, and Yu Su. GPT-4V(ision) is a Generalist Web Agent, if Grounded. *arXiv preprint*, 2024. 1

A. GUI navigation tasks

Android In The Wild (AITW) [37] consists of 30k instructions and 715k operation trajectories in the context of smartphone environments. However, the original training split carries the risk of overfitting due to overlapping instructions between the training and test sets, as well as the presence of multiple similar trajectories per instruction [6]. Therefore, we adopt the instruction-wise split scheme proposed by SeeClick [6] for the AITW dataset to achieve a fair evaluation. We follow the same data processing settings in SeeClick. The action space of AITW consists of 12 actions: CLICK, TYPE, SELECT, SCROLL UP, SCROLL DOWN, SCROLL LEFT, SCROLL RIGHT, PRESS BACK, PRESS HOME, PRESS ENTER, STATUS TASK COMPLETE, STATUS TASK IMPOSSIBLE.

Mind2Web [9] comprises over 2000 open-ended tasks collected from 137 real websites, originally for text-based web agents, provides only HTML observations. To support visual agents, we extracted screenshots and target bounding boxes. Since full-page captures (e.g. 1920×12000) are impractical for LVLMs, we follow the same data processing settings in SeeClick, cropping around target elements, standardizing the resolution to 1920×1080. The action space of Mind2Web consists of 2 actions: CLICK, TYPE.

GUI-Odyssey [29] is a comprehensive dataset for training and evaluating cross-app navigation agents, consisting of 7,735 episodes from 6 mobile devices. We follow the same data processing and evaluation settings in GUI-Odyssey. The action space of GUI-Odyssey consists of 9 actions: CLICK, SCROLL, LONG PRESS, TYPE, COMPLETE, IMPOSSIBLE, HOME, BACK, RECENT.

AndroidControl [18] encompasses 14,548 unique tasks across 833 Android apps, offering both high and low-level instructions to explore the level of task complexity an agent can handle. We follow the same data processing and evaluation settings in OS-Atlas [54]. The action space of AndroidControl consists of 9 actions: CLICK, SCROLL, LONG PRESS, TYPE, NAVIGATE HOME, NAVIGATE BACK, OPEN APP, WAIT, TERMINATE.

B. Implementation Details

We use Qwen2VL-2B as our base model. For different datasets, we adopt the same data organization format following SeeClick [6]. We parse the executed actions in JSON format, dividing them into two parts: `action_type` and `action_value`. Next, we introduce the format and examples of the training and testing data.

For the 4A data format, we use the same prompt in SeeClick to execute each step of the agent.

```
"<image>Please generate the next move according to the ui screenshot, instruction and previous actions.
Instruction: What's on the menu at Domino's?.
Previous actions:
Step0: {"action_type": PRESS HOME}.
Step1: {"action_type": CLICK, "click_point": (524,865)}.
Step2: {"action_type": TYPE, "typed_text": "menu at Domino's"}.
Step3: {"action_type": CLICK, "click_point": (325,156)}. "
```

For the 4AO data format, we use the following prompt to execute each step of the agent.

```
"Please generate the next move according to the instruction, previous actions, previous ui screenshot and current ui screenshot.
Instruction: What's on the menu at Domino's?.
Image_0:<image>
Step_0:{"action_type": PRESS HOME} .
Image_1:<image>
Step_1:{"action_type": CLICK, "click_point": (524,865)} .
Image_2:<image>
Step_2:{"action_type": TYPE, "typed_text": "menu at Domino's"}.
Image_3:<image>
Step_3:{"action_type": CLICK, "click_point": (325,156)} .
Image_4:<image> "
```

For the AITW [37] and GUI-Odyssey [29] datasets, we employ four low-resolution historical images, adhering to the 4AO format proposed by SeeClick. Each image's longest side is scaled to 512 pixels, maintaining the aspect ratio and ensuring the resolution stayed within 512×512.

For AndroidControl [18] and Mind2Web [9] datasets, we adopt the same setting in ShowUI, retaining two high-resolution historical images, with a maximum of 1280 tokens. We choose not to use four due to GPU memory constraints.

We use bfloat16 precision for training. All experiments are conducted with LoRA fine-tuning, applying a rank of 8 and an alpha value of 16 exclusively for the language model. We leverage DeepSpeed Zero-2 and utilize flash attention to accelerate training. For AITW and GUI-Odyssey, we use the same training strategy in SeeClick, with a learning rate of 3e-5 and a global batch size of 64. For AndroidControl, we use a learning rate of 3e-4 and a global batch size of 128. For Mind2Web, we use a learning rate of 3e-4 and a global batch size of 16.

C. The statistical Analyses of GUI Navigation Datasets

In Figure 8, We present the distribution of the element nums included in screenshots from the AITW dataset. The number of elements per screenshot typically falls within the range of 10 to 100, reflecting the characteristic of GUI scenes having a large number of visual elements.

In Figure 9, we present the distribution of the target element ratio in the Mind2Web dataset. It is evident that most

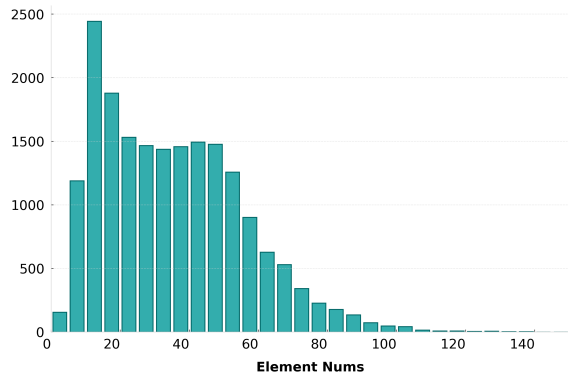


Figure 8. The distribution of element nums in AITW dataset.

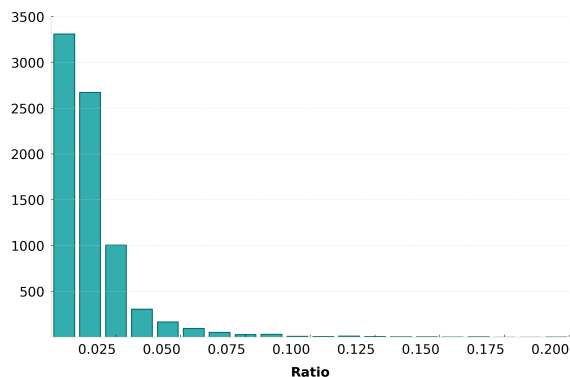


Figure 9. The distribution of target element ratio in Mind2Web dataset.

elements occupy less than 3% of the entire screen, a characteristic that contributes to the difficulty in element localization in GUI scenes.

D. More detailed results

In Tables 8, 9, 10, we present the performances on all subsets of each navigation dataset. On AITW (6.5 steps on average), our SimpAgent significantly outperforms ShowUI, except the “Single” subset (1.5 steps on average). We attribute it to the large-scale grounding pre-training of ShowUI, which enhances its single-horizon task completion ability. On GUI-Odyssey (15.4 steps on average), SimpAgent achieves the performance gains of 3.41% on the “Multi-Apps” subset (22.3 steps on average), 3.58% on the “Shopping” subset (18.2 steps on average), demonstrating its superior ability of accomplishing long-horizon tasks. On Mind2Web, our SimpAgent and SimpAgent-M produce new state-of-the-art performances on three out-of-domain test sets. Our SimpAgent-M is slightly inferior to SimpAgent and comparable with the baseline Qwen2VL on the “Cross-Website” test set, and the performance gap is relatively small. We speculate that the insignificant performance difference may be due to the limited size of the “Cross-Website” set (only 177 tasks), which is insufficient

to yield reliable experimental conclusions.

E. Case Study

In Figure 10, we present more navigation tasks. The baseline model (fine-tuned Qwen2-VL) is unable to complete these steps. In contrast, the visualizations show that our SimpAgent can effectively reduce interference and correctly identify relevant elements while ignoring irrelevant ones. In Figure 11, we present more cases about the attention difference between w/ and w/o consistency guidance. These visualizations demonstrate that the historical action tokens pay more attention to the adjacent historical vision tokens under the setting of consistency guidance, facilitating a better information aggregation. In Figure 12 and 13, we present the complete task execution trajectory of SimpAgent.

Method	#P.T.	#Param.	General	Install	GoogleApps	Single	WebShopping	Overall
GPT-4V [32]	-	-	41.7	42.6	49.8	72.8	45.7	50.5
QwenVL [1]	-	9.6B	49.5	59.9	46.9	64.7	50.7	54.3
SeeClick [6]	850K	9.6B	54.0	66.4	54.9	63.5	57.6	59.3
Qwen2VL* [47]	-	2B	59.4	71.7	64.2	71.8	63.0	66.0
Qwen2VL [47]	-	2B	61.2	73.5	72.1	73.8	64.2	69.0
Iris [10]	850K	9.6B	61.5	71.4	58.3	66.4	60.2	63.6
ShowUI [25]	256K	2B	63.9	72.5	69.7	77.5	66.6	70.0
SimpAgent	-	2B	64.3	75.5	73.7	75.8	67.0	71.3
SimpAgent-M	-	2B	64.1	75.8	74.0	76.2	67.2	71.5

Table 8. Step success rate on AITW, divided by domains. “#P.T.” and “#Param.” denote the number of pre-training GUI datasets and parameters, respectively. “*” means the variant utilizing only action history. “-M” denotes only applying masking-based element pruning without inference FLOPs reduction.

Method	#Param.	Cross-Task			Cross-Website			Cross-Domain		
		Ele.Acc	Op.F1	Step SR	Ele.Acc	Op.F1	Step SR	Ele.Acc	Op.F1	Step SR
Qwen-VL [1]	9.6B	15.9	86.7	13.3	13.2	83.5	9.2	14.1	84.3	12.0
CogAgent [12]	18B	22.4	53.0	17.6	18.4	42.4	13.4	20.6	42.0	15.5
SeeClick [6]	9.6B	28.3	87.0	25.5	21.4	80.6	16.4	23.2	84.8	20.8
Qwen2VL* [47]	2B	49.7	89.1	45.0	46.8	86.5	40.9	45.4	86.6	40.5
Qwen2VL [47]	2B	51.6	88.6	46.7	48.5	85.7	42.2	48.3	87.0	44.6
Iris [10]	9.6B	33.5	87.1	32.0	31.2	82.2	26.2	32.8	85.1	28.8
ShowUI [25]	2B	39.9	88.6	37.2	41.6	83.5	35.1	39.4	86.8	35.2
SimpAgent	2B	51.0	89.2	47.1	48.7	86.0	42.8	46.9	86.5	43.3
SimpAgent-M	2B	52.4	89.4	48.7	48.2	85.8	42.2	49.0	88.2	45.0

Table 9. Performance comparison on Mind2Web across different settings. We report element accuracy (Ele.Acc), operation F1 (Op.F1), and step success rate (Step SR). “#Param.” denotes the number of parameters. “*” means the variant utilizing only action history. “-M” denotes only applying masking-based element pruning without inference FLOPs reduction.

Method	#P.T.	#Param.	Tool	Information	Shopping	Media	Social	Multi-Apps	Overall
GPT-4V [32]	-	-	23.49	20.16	19.15	16.92	13.83	19.02	18.76
GPT-4o [15]	-	-	20.81	16.28	31.91	15.38	21.28	16.67	20.39
CogAgent [12]	140M	18B	15.66	10.74	9.15	11.66	13.08	10.73	11.84
QwenVL [1]	-	9.6B	83.11	65.70	62.43	76.38	76.12	73.10	72.81
Qwen2VL* [47]	-	2B	80.35	62.42	59.52	71.11	72.75	67.91	69.01
Qwen2VL [47]	-	2B	83.71	67.44	64.79	77.19	79.08	76.97	74.86
OdysseyAgent [29]	-	9.6B	85.16	68.53	62.87	76.49	77.61	74.83	74.25
SimpAgent	-	2B	84.91	69.89	66.45	78.05	79.21	78.24	76.02
SimpAgent-M	-	2B	86.57	70.08	67.65	79.78	81.04	79.21	77.39

Table 10. Step success rate on GUI-Odyssey Test-Random split. “#P.T.” and “#Param.” denote the number of pre-training GUI datasets and parameters, respectively. “*” means the variant utilizing only action history. “-M” denotes only applying masking-based element pruning without inference FLOPs reduction.



Figure 10. Illustration of navigation steps in the GUI-Odyssey dataset. SimpAgent distinguishes the correct element among various confusing elements. This demonstrates the effectiveness of our proposed Masking-based Element Pruning method.

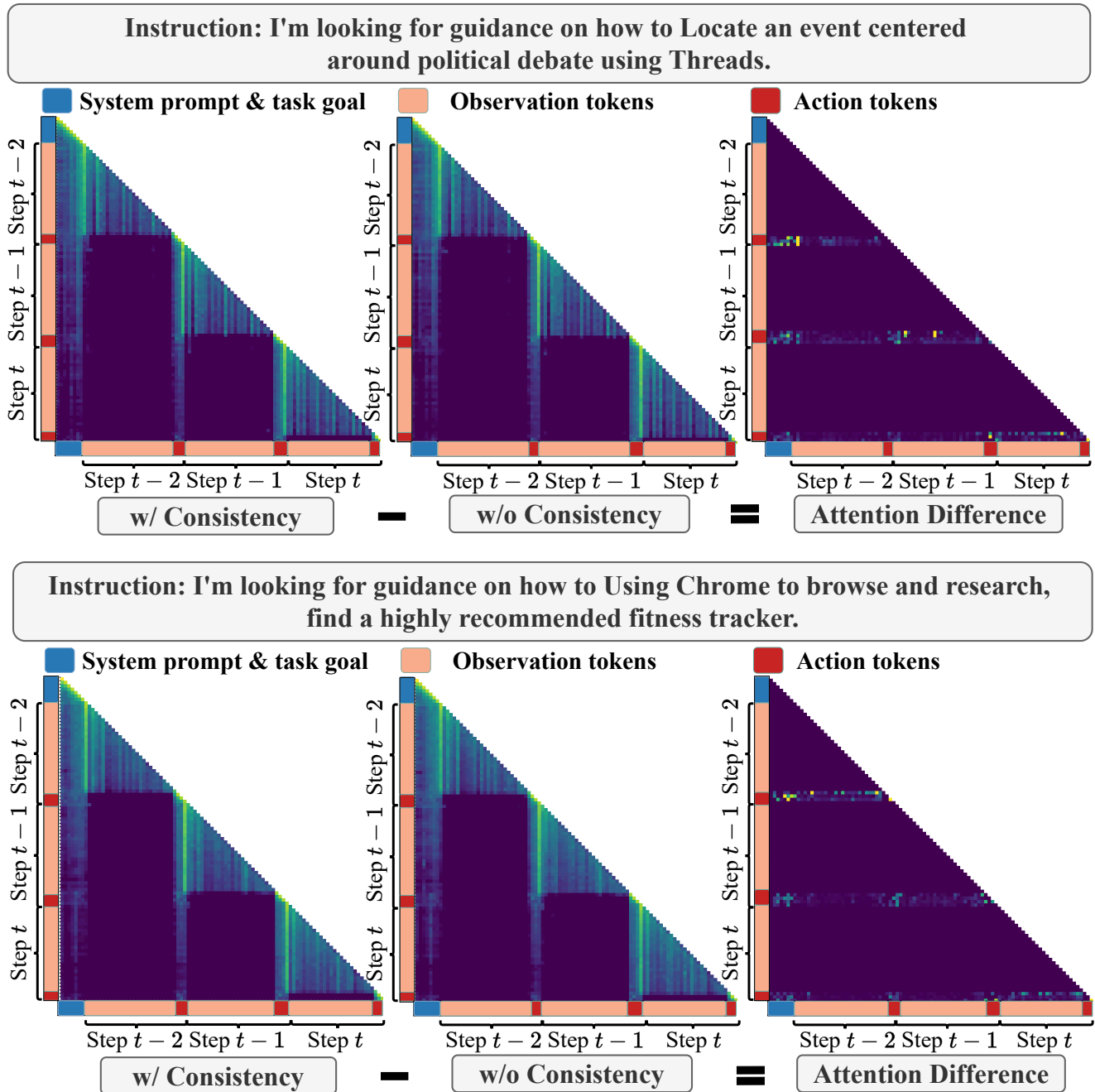


Figure 11. Illustration of attention maps in agent models w/ and w/o consistency guidance, and their attention difference map. The **attention difference map** shows that action tokens pay more attention (highlighted positions) to historical observation tokens when they act as query tokens with consistency guidance. This attention comparison demonstrates that consistency guidance can promote the information aggregation from observations to actions and facilitate the history compression.

Instruction: Calculate the fare options to go from the south station to the north station.

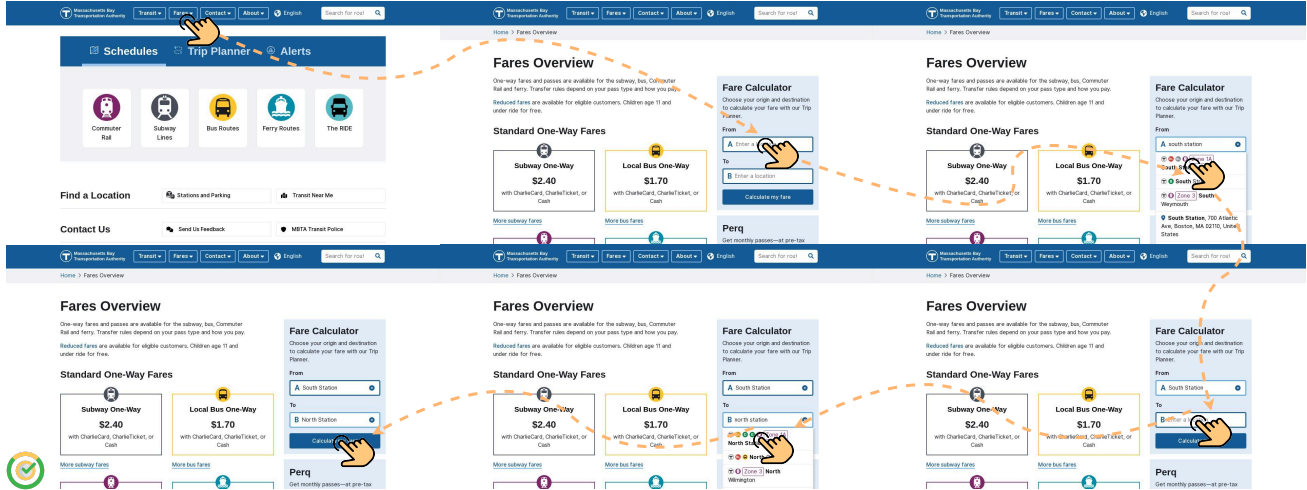


Figure 12. The real-world application of SimpAgent when adapted to downstream GUI navigation tasks.

Instruction: Find a Lenovo laptop under \$800 and create a price alert for 400\$.

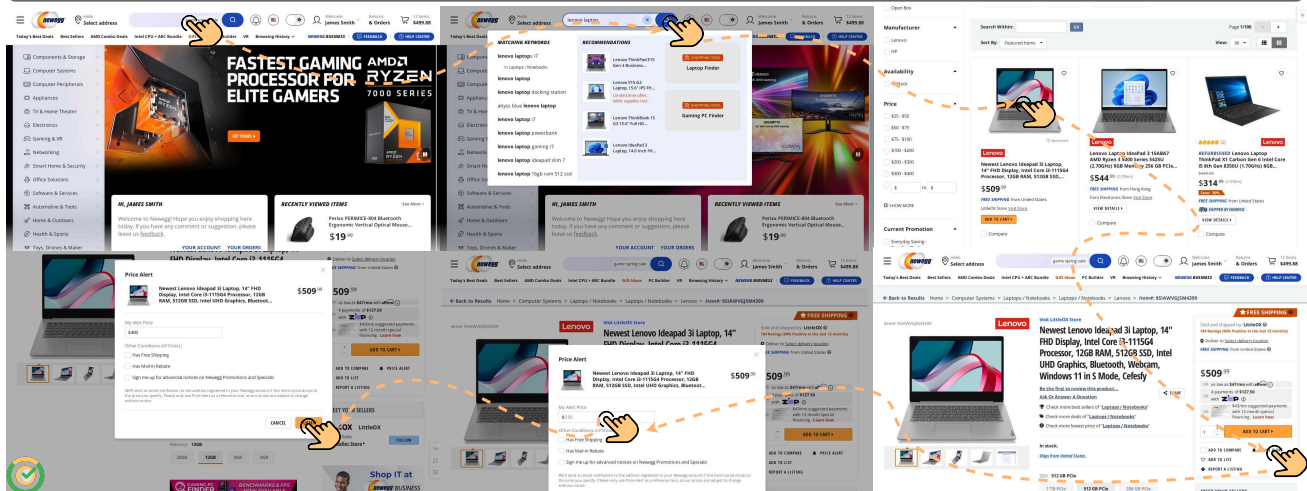


Figure 13. The real-world application of SimpAgent when adapted to downstream GUI navigation tasks.